ICES Journal of Marine Science, 60: 625–635. 2003
doi:10.1016/S1054–3139(03)00063-8

Validation of the stochastic distorted-wave Born approximation model with broad bandwidth total target strength measurements of Antarctic krill

David A. Demer and Stéphane G. Conti

Demer, D. A., and Conti, S. G. 2003. Validation of the stochastic distorted-wave Born approximation model with broad bandwidth total target strength measurements of Antarctic krill. – ICES Journal of Marine Science, 60: 625–635.

Total-scattering cross-sections (σ_t) of Antarctic krill (*Euphausia superba*) were measured over a broad bandwidth (36–202 kHz) using a new technique based on acoustical reverberation in a cavity. From 18 February to 9 March 2002, mean total target strengths ($TTS = 10\log(\sigma_t/4\pi)$), were measured from groups of 57–1169 krill (average standard length = 31.6 mm; standard deviation = 6.6 mm) at the Cape Shirreff field station, Livingston Island, Antarctica, and aboard RV "Yuzhmorgeologiya". Chirp pulses were transmitted sequentially by an omni-directional emitter into one of three glass carboys containing groups of krill swimming in 9.3, 19.3, or 45.9 liters of seawater ($0.6°C \leq$ temperature $\leq 4.0°C$). Between each pulse the krill moved within the fixed-boundary tank and the modulated reverberations were sensed bi-statically with three omni-directional receivers. At each center frequency (f_c), the coherent energy in 200-pulse ensembles identified sound scattered by the tank. The incoherent energy described total sound scattering from the krill. Thus, the TTS at each f_c was extracted from a correlation analysis of energy reverberated in the tank. Measurement bias was determined to be ± 0.4 dB from an experiment using metal sphere reference targets, and the precision was estimated as ± 0.8 dB from the variability in the krill TTS (f_c) measurements. The empirical estimates of mean σ_t corroborated a krill-scattering model based on the distorted-wave Born approximation (DWBA), enhanced by the authors to account for the stochastic nature of sound scattering (SDWBA), integrated over all scattering angles and averaged over all incident angles ($SDWBA_{TTS}$). The SDWBA, solved for target strength of Antarctic krill, may be the best predictor of backscatter for this important species and may also provide backscattering spectra for improving their acoustic identification. These advances may help to reduce uncertainty in krill-biomass estimation using multi-frequency echosounder data and echo-integration methods.

Published by Elsevier Science Ltd on behalf of International Council for the Exploration of the Sea.

Keywords: Antarctic krill, broadband, classification, stochastic distorted-wave Born-approximation model, total cross-section, total target strength.

D. A. Demer and S. G. Conti: Southwest Fisheries Science Center, 8604 La Jolla Shores Drive, La Jolla, CA 92037, USA; e-mail: stephane.conti@noaa.gov. Correspondence to D. A. Demer; tel:/fax: +1 858 546 5603/8; e-mail: David.Demer@noaa.gov.

Introduction

The United States of America's Antarctic Marine Living Resources Program (AMLR) uses multi-frequency echosounders and echo-integration to map the dispersion of Antarctic krill (*Euphausia superba*) over large areas and to estimate their abundance (Hewitt and Demer, 2000). The bias and precision of the survey results depend primarily on the uncertainties in identifying acoustical backscatter from krill and in estimating the mean backscattering cross-section (σ), or target strength ($TS = 10\log(\sigma)$) of krill (Demer, in press).

Model estimates of TS are based either on empirical data or on the physics of sound scattering. For Antarctic krill, Greene *et al.* (1991) proposed a linear model of TS versus total length (L), based on measurements of various crustacean zooplankton (Wiebe *et al.*, 1990) and corroborated at frequency f = 120 kHz for krill over a small range of L (Foote *et al.*, 1990; Hewitt and Demer, 1991). The implications of using the Greene *et al.* model were explored (Everson *et al.*, 1990) and the model was adopted as an international standard for estimating krill biomass (CCAMLR, 1991).

Taking the physics-based approach, McGehee *et al.* (1998) used the distorted-wave Born approximation (DWBA; Morse

and Ingard, 1968) to model the TS of krill versus f, and animal body-mass density (ρ), sound speed (c), L, shape (s), and angle of orientation relative to the incident wave (Φ). The krill s is modeled as a string of cylinders having varying diameters and positions along a curve, and TS is estimated from a coherent summation of backscatter from these elements. With TS(Φ) measurements of tethered, live krill in a tank, they validated the DWBA model near broadside incidence (ca. $75^\circ \leq \Phi \leq 105^\circ$) at $f = 120$ kHz. However, there was poor agreement between the DWBA and their TS measurements for Φ away from the main lobe. Demer and Conti (2003) developed a stochastic version of the DWBA (SDWBA) that models the effects of animal flexure, shape complexities, and noise with a random-phase term for each of the cylinders. The resulting degree of incoherence explains the discrepancies between McGehee *et al.*'s empirical data and theory over all angles of incidence (or krill orientation).

It is now desirable to gather empirical corroboration of the new SDWBA model over a broad bandwidth. Unfortunately, the constraints of conventional techniques for making free-field measurements of krill TS with a broad bandwidth and known distributions of animal sizes and orientations make this a formidable challenge (see Demer *et al.*, 1999; Ona, 1999). Recently, however, a new technique has been developed (De Rosny and Roux, 2001) for conveniently and accurately (Demer *et al.*, 2003) making broad-bandwidth measurements of total scattering cross-sections (σ_t), or total target strength ($TTS = 10\,log(\sigma_t/4\pi)$) of one or more scatterers moving in an echoic cavity with static boundaries.

Contrary to the free-field requirement of conventional TS-measurement techniques, the new method extracts measurements of TTS from quotients of the incoherent and coherent energies in ensembles of reverberation time-series. Also intriguing is that absolute measurements of sound scatter can be made without the usual system calibration—the system parameters cancel in the quotient—and the animals' orientations and positions within the acoustical beam are inconsequential because the reverberant sound field is homogeneous. By employing this novel method, the aims of our investigation are: (1) to make broad-bandwidth TTS measurements of swimming krill; (2) to use these measurements to validate the SDWBA model over a broad bandwidth (the SDWBA model can be evaluated for TS ($SDWBA_{TS}$) and TTS ($SDWBA_{TTS}$)); and (3) thus provide both an improved tool for predicting krill TS, and a broad-bandwidth spectrum for acoustically identifying krill.

Methods

Empirical TTS of Antarctic krill

From 18 to 24 February 2002, TTS measurements of Antarctic krill were made at AMLR's Cape Shirreff field station on Livingston Island, Antarctica. Details of the general processing steps are outlined in De Rosny and Roux (2001) and Demer *et al.* (2003). Descriptions of the equipment and procedures specific to these measurements follow.

The krill were captured near the South Shetland Island archipelago using a 2-m Isaacs–Kidd midwater trawl (IKMT), deployed from RV "Yuzhmorgeologiya". They were kept alive and transferred ashore via Zodiac in 20 liter buckets of seawater. For each experiment, a glass carboy ($9.3 \pm 2\%$, $19.3 \pm 1.6\%$, or $45.9 \pm 0.9\%$ liter) was filled completely with ambient seawater at temperatures ranging from 0.6 to 4.0°C. Groups of 57–1169 krill were then added and the top was closed with a rubber stopper containing an emitter, three receivers, and a thermocouple (Figure 1). Displacing small amounts of water in the process, the resultant cavity had no air–water interface. This setup and procedure provided an echoic cavity with fixed boundaries, a requisite while conducting the experiments on a moving ship. From 26 February to 9 March, the TTS measurements were continued aboard AMLR's chartered RV "Yuzhmorgeologiya".

At center frequencies (f_c) ranging from 36 to 202 kHz, frequency-modulated pulses (0.4 V_{p-p}; 500 μs) with a 2 kHz bandwidth were generated (Hewlett Packard 33120A arbitrary-waveform generator), amplified 20 dB (Krohn-Hite 7500 power amplifier), and transmitted twice-per-second using an omni-directional, broad-bandwidth emitter and received bi-statically with three omni-directional broad-bandwidth receivers. During sequential pulses ($k = 1$–200), the animals moved within the fixed-boundary tank and $t = 0$ to 10, 20, or 32 ms of the modulated reverberation ($h_k(t)$) were digitized at 410 kHz using a 12-bit analog-to-digital converter (National Instruments Daqpad 6070E). The lengths of the recorded time-series depended on the signal-to-noise ratio (SNR) and thus mainly on the carboy volume and the number of krill therein (see Table 1). To reduce noise, the $h_k(t)$ were match-filtered by cross-correlation with the transmitted signal. The coherent energy in 200-pulse ensembles identified sound scattered from the echoic tank. Because the positions of the animals were uncorrelated from ping-to-ping, the incoherent energy described sound scattering from the krill. The ratio of uncorrelated ($\langle h_k(t) h_{k+1}(t) \rangle$) and correlated ($\langle h_k(t)^2 \rangle$) energies decayed exponentially:

$$S(t) = \left(\frac{\langle h_k(t) h_{k+1}(t) \rangle}{\langle h_k(t)^2 \rangle} \right). \quad (1)$$

The exponential decay of S(t) was estimated for each 200-pulse ensemble by separately low-pass filtering the numerator and denominator in the linear domain ($f_{cutoff} = 500$ Hz), and fitting a least-squares slope ($d\ln(S(t))/dt$), while requiring $2 \leq t \leq 9$ ms for the 9.3 and 19.3 liter cavities, $3 \leq t \leq 13$ ms for the 45.9 liter cavity, and $\ln(S(t)) = 0$ at $t = 0$. Knowing the volume of the cavity (v), the number of krill (n), and the sound speed in seawater (c), an estimate of σ_t was made for each group of krill and f_c:

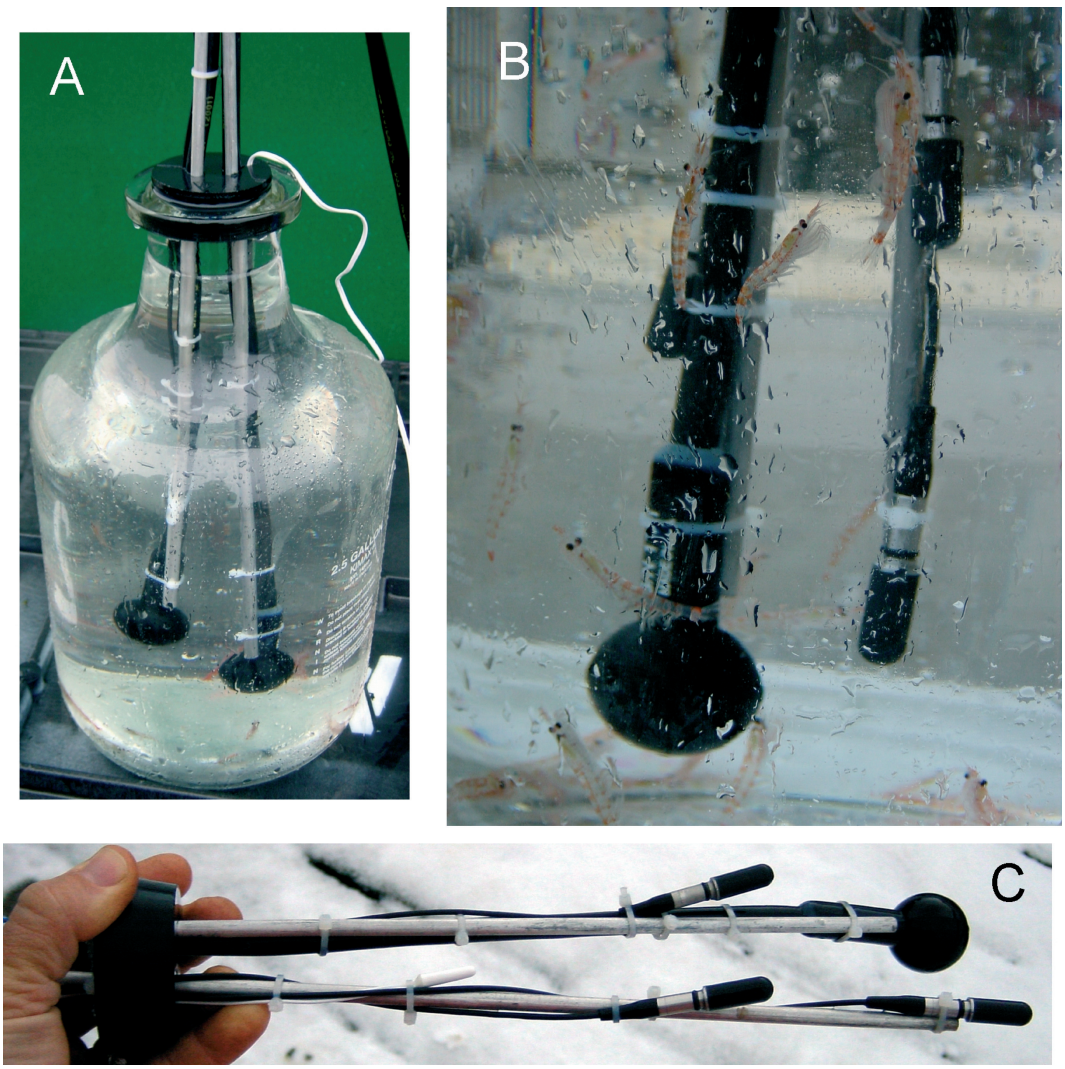

Figure 1. (A) An echoic glass carboy as used for broad-bandwidth TTS measurements of krill. (B) Krill swimming in the $19.3 \pm 1.6\%$ liter carboy aboard RV "Yuzhmorgeologiya". (C) A rubber stopper fitted with the omni-directional emitter (ITC 1042), three omni-directional receivers (Reson TC4013), and a thermocouple for a digital thermometer (RS/63-1009A). A third carboy ($45.9 \pm 0.9\%$ liter) was also used but is not shown.

$$\sigma_t \approx -\frac{v}{cn}\frac{d\ \ln(S(t))}{dt}. \qquad (2)$$

Thus, TTS(f) measurements were made of 12 aggregations of 57–1169 swimming krill (Table 1) from the reverberation sensed at three receiver locations, and during one or more 3-h runs. Following the measurements of each aggregation, L was measured to the nearest millimeter (from the anterior tip of the rostrum and the posterior end of the uropods, excluding their terminal setae) before preserving in sample jars with ethanol.

Demer *et al.* (2003) used precision metal spheres to demonstrate that this TTS-measurement technique is remarkably accurate (± 0.4 dB) and precise (± 0.7 dB). However, v should not be too large compared to the total volume of the scatterers; the reflectivity of the boundaries must be high and the reverberation time-series must be long enough to precisely estimate $d\ \ln(S(t))/dt$. Also, a large number of modes must be excited in the cavity to obtain a homogeneous sound field. As a guideline limit, $v \geq 100\lambda^3$ ($\lambda = c/f$), or $v \geq 7$ liter at 36 kHz (De Rosny and Roux, 2001). Thus, the working bandwidth in these experiments was limited by the reflectivity of the glass carboys and the frequency responses of the emitter and receivers.

Theoretical TTS of Antarctic krill

To predict the empirical estimates of σ_t, the SDWBA model was integrated over all scattering angles and averaged over

Table 1. Metadata for the first TTS measurements of Antarctic krill.

Experiment date	Measurement location	Tank volume (l)	No. of krill (n)	Record length (ms)	Water temp. (°C)
21 Feb 2002	Cape Shirreff	9.3	302	20	3.6
22 Feb 2002	Cape Shirreff	9.3	100	20	1.6
23 Feb 2002	Cape Shirreff	9.3	57	20	3.4
24 Feb 2002	Cape Shirreff	19.3	57	20	4.0
26 Feb 2002	RV "Yuzhmorgeologiya"	45.9	1169	32	3.7
27 Feb 2002	RV "Yuzhmorgeologiya"	19.3	326	20	2.0
8 Mar 2002	RV "Yuzhmorgeologiya"	19.3	258	10	0.6
8 Mar 2002	RV "Yuzhmorgeologiya"	9.3	152	10	2.5
8 Mar 2002	RV "Yuzhmorgeologiya"	9.3	86	10	3.4
9 Mar 2002	RV "Yuzhmorgeologiya"	19.3	173	10	1.4
9 Mar 2002	RV "Yuzhmorgeologiya"	9.3	176	10	2.3
9 Mar 2002	RV "Yuzhmorgeologiya"	19.3	117	10	3.1

all incidence angles ($SDWBA_{TTS}$). The computation is detailed in Appendix A. Parameters include the generic krill shape (McGehee *et al.*, 1998), $c = 1455\ m\ s^{-1}$, the non-dimensional sound-speed and density contrasts ($h = 1.0279$ and $g = 1.0357$, respectively) from Foote (1990) and Foote *et al.* (1990), and random phase chosen from a normal distribution $(\varphi = N[0°, 40.5°])$ from Demer and Conti (2003). The generic krill shape, derived for a krill with $L = 38.35$ mm, was proportionately scaled to represent the smaller krill in these experiments (average $L = 31.6$ mm). Thus, $SDWBA_{TTS}$ was evaluated from 36 to 202 kHz.

Results

The mean TTS of Antarctic krill was measured acoustically over a broad bandwidth (36–202 kHz), on land and at sea, from 18 February to 9 March 2002 (Figure 2). By match-filtering the reverberation time-series to reduce noise (e.g. from the ship and the electronics), the TTS measurements made aboard RV "Yuzhmorgeologiya" were comparable to those made at Cape Shirreff. In general, the TTS measurements increased monotonically versus f with a gradual reduction in slope. In 9 of 12 runs, the $TTS(f_c)$ from about 90 to 202 kHz showed remarkable agreement with the $SDWBA_{TTS}$ calculated for the mean L in each aggregation. The TTS measurements from two of the aggregations, 117 and 326 krill, respectively, were, in fact, nearly identical matches to the $SDWBA_{TTS}$ over the entire measurement bandwidth.

Anomalous increases in TTS below about 150 kHz occurred in the measurements with 86 and 173 krill (Figure 2). This is true, but to a lesser extent, for the measurements with 176 krill. This characteristic is probably an artifact of residual aeration in the carboy at the beginnings of the runs. As f_c was scanned from 36 to 202 kHz over about 3 h, the uncorrelated bubble scatter diminished over time and did not bias the results at higher frequencies.

The TTS measurement precision (s.d.) is estimated as ±20% (±0.8 dB) from three recordings per krill aggregation. Judging from Demer *et al.* (2003), the systematic error of these krill TTS measurements could be estimated as ±0.4 dB. However, because krill are weaker scatterers, and the cavity volumes were smaller than for the standard-sphere measurements, some additional measurement bias might be expected, especially at the lower frequencies.

The krill length-frequencies were variable between aggregations and varied from quasi-uniform to normal distributions (Figure 3). The overall distribution was negatively skewed with lengths ranging between approximately 20 and 50 mm (mean $L = 31.6$ mm; s.d. $= 6.6$ mm).

A mean TTS spectrum was obtained by averaging the results of the individual runs, excluding the measurement from the 86 and 173 krill (Figure 4). Despite the omission of the two anomalously noisy data sets, the slope of $TTS(f_c)$ is questionably flat below about 60 kHz. This feature, and decreasing SNR below about 80 kHz as indicated by virtually identical reverberation time-series for all the pings within an ensemble, suggests that the measurements at frequencies $f_c = 38$ to 58 kHz are unreliable and those between 60 and about 80 kHz may have a small positive bias due to noise. The 1- to 2-dB spike in the TTS measurements from 196 to 200 kHz was observed in all the runs and may be an artifact of the cavity geometry and hydrophone placement.

The mean krill TTS were compared to the $SDWBA_{TTS}$ calculated with the L probability density function for all the measured krill (Figure 3). Considering mean TTS from $f_c = 60$ to 202 kHz, the measurements ranged from about −84.6 to −71.0 dB, and their ±1 s.d. lines encompass the $SDWBA_{TTS}$ predictions (Figure 4). Over the same range of f, the predicted TTS ranges from about −85.6 to −72.0 dB. The two curves match to within a fraction of 1 dB from 60 to about 130 kHz, and within 1 dB at higher frequencies.

Discussion

The currently accepted model for krill TS (Greene *et al.*, 1991), which depends linearly only on log(L), was developed empirically for $f = 420$ kHz, and is scaled to different f assuming a frequency-squared relationship.

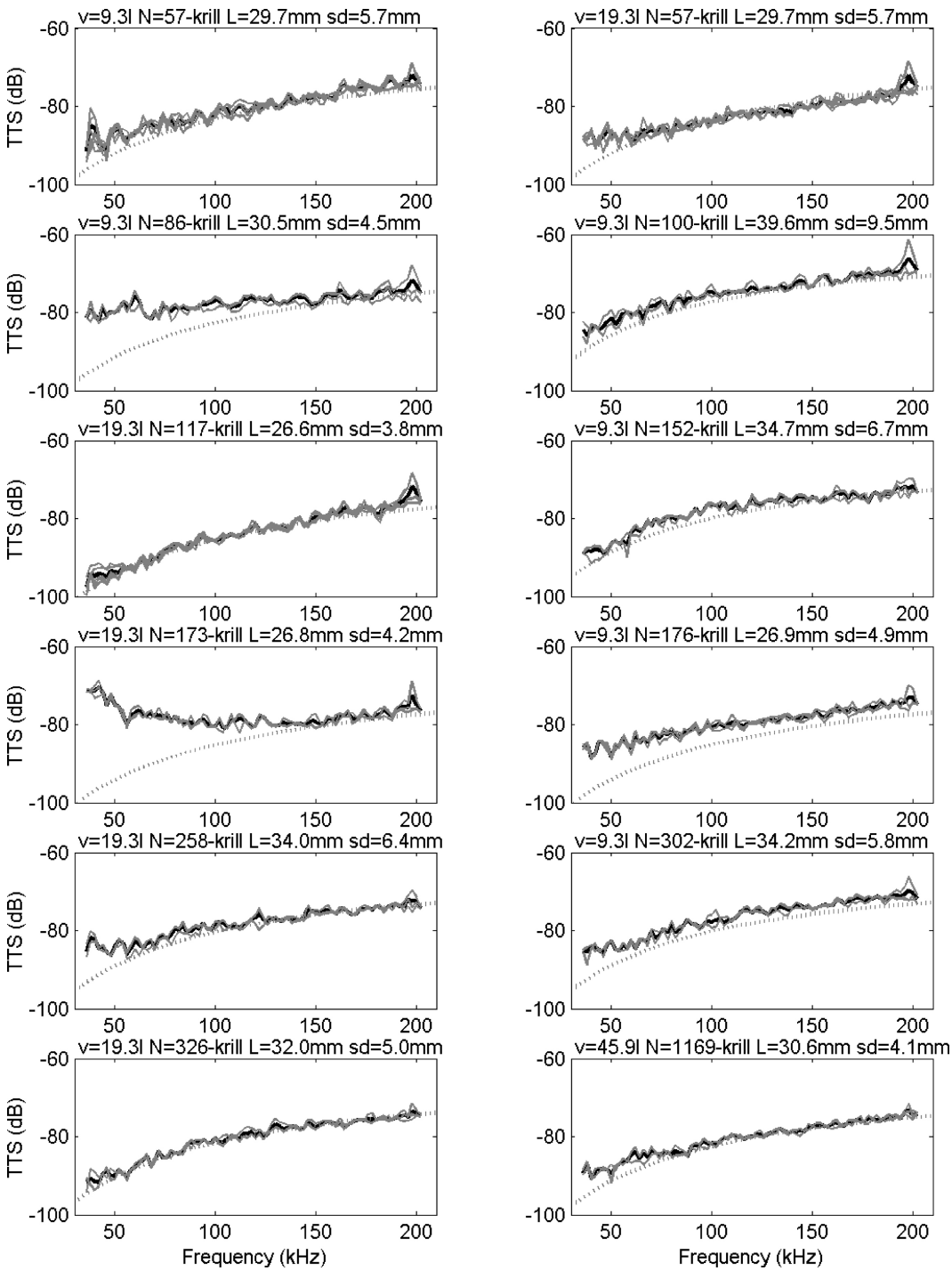

Figure 2. Mean TTS of *Euphausia superba* measured from aggregations totaling 57–1169 animals. For each run, the spectra were recorded with three hydrophones at different positions in the carboy. Two runs were recorded for some aggregations. To demonstrate the negligible effect of the cavity volume, the same 57 krill were recorded in both the 9.7 and 19.3 liter carboys (top panels).

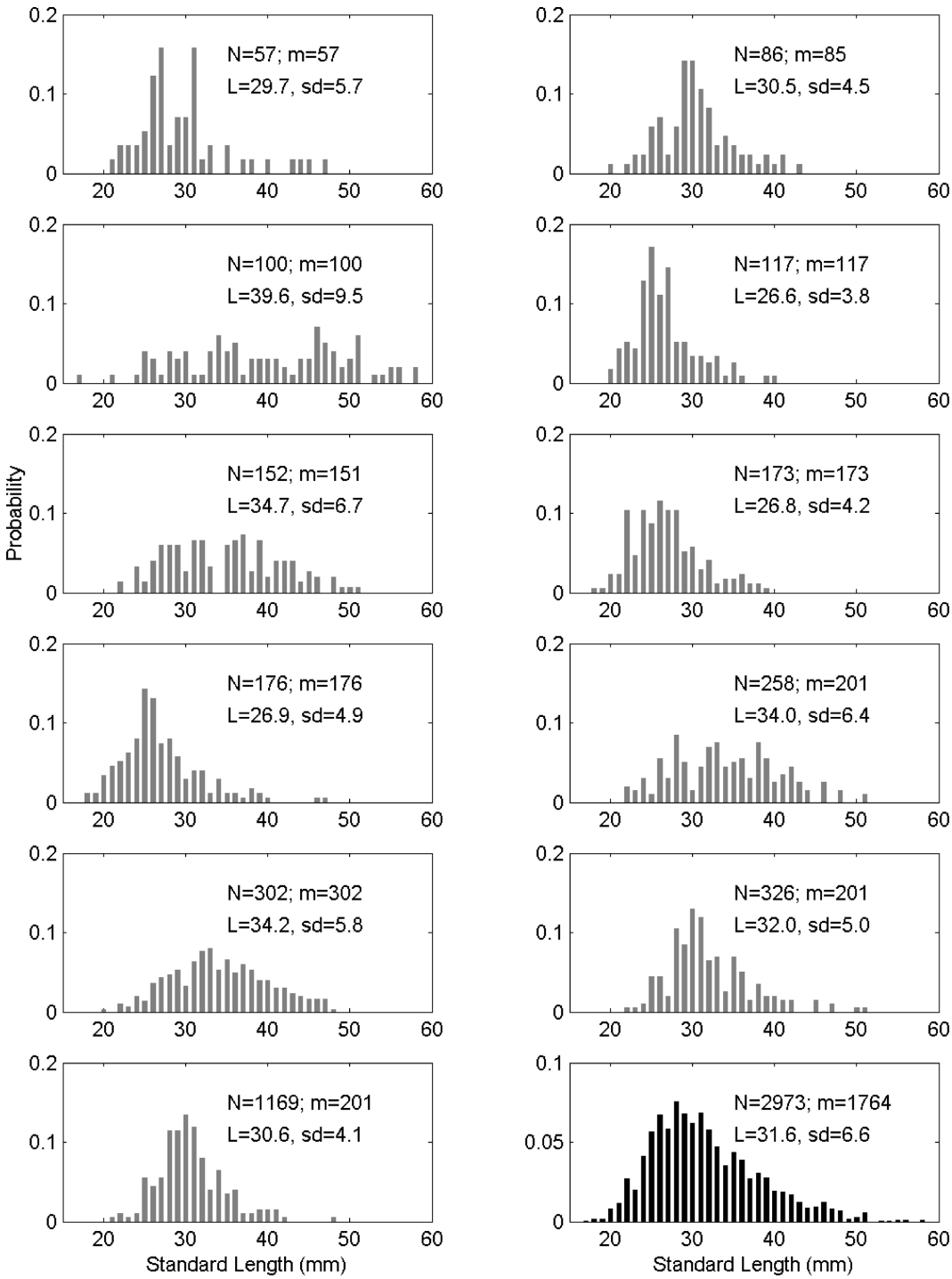

Figure 3. Krill length-frequencies are shown for each batch of krill (gray) and all of the krill combined (black). Labeled for each experiment are the number of krill (*N*), the number of krill lengths measured (m), the mean total length (L), and the standard deviation (s.d.).

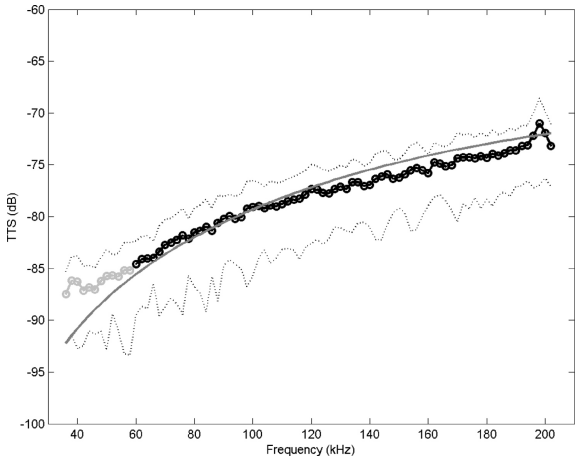

Figure 4. The average TTS of 10 aggregations of *Euphausia superba* totaling 57–1169 animals. TTS data from 36 to 60 kHz had low SNRs (gray circles); those above 60 kHz are considered accurate to about 0.4 dB (black circles). The ±1 s.d. error bands (dashed lines) encompass the $SDWBA_{TTS}$ predictions (solid gray), computed with g = 1.0357, h = 1.0279, generic s, and the overall krill length-frequency distribution (see Figure 3). Because the random-phase term caused variations in $SDWBA_{TTS}$ of less than 0.1 dB, expected values of TTS were effectively computed at each f using only a single random realization of phase. Error bounds on the prognosticator are thus negligible.

However, the krill TTS measurements in this study do not indicate a strong linear relationship between scattering intensity and animal length (see Figure 5 and note the frequency-dependent slopes, y-intercepts, and low R^2 values). Also, for a given L, krill shapes, volumes, and material properties can be dramatically variable. Moreover, krill orientation has a dominant effect on TS variability (see Demer and Martin, 1995), and both gender and maturation state affect Φ. For example, mature female krill with swollen cephalothoraxes are thought to have larger tilt angles than males (Endo, 1993).

The DWBA model (McGehee *et al.*, 1998) accounts for all these parameters (i.e. TS(f, c, g, h, s, L, Φ)). Lavery *et al.* (2002) developed another version of the DWBA that replaces the generic krill shape (McGehee *et al.*, 1998) with high-resolution, three-dimensional measurements of the animal's exterior boundary. However, in view of the uncertainties associated with the other model parameters, animal flexure and motion, and the animal-to-animal variability in s, this degree of model complexity may provide little practical improvement, especially at lower frequencies.

Demer and Conti (2003) accounted for the stochastic nature of sound scattering in a model that provides probabilities of krill TS versus all angles of orientation (SDWBA). The SDWBA has now been corroborated with TTS over a broad range of frequencies and can easily accommodate distributions of animal density and sound speed contrasts, shape, size, and orientations, assuming they can be characterized. For very high frequencies it can also be extended to three-dimensional shapes (viz. Lavery *et al.*, 2002).

To predict σ or TS for Antarctic krill, the expected value of $SDWBA_{TS}$ was estimated as a function of f_c and L (Figure 6). As in Demer and Conti (2003). $SDWBA_{TS}$ was averaged over 100 realizations computed with inter-element phase variability ($\varphi = N[0°,\ 40.5°]$), and over the Gaussian krill-orientation distribution from Kils (1981); ($\Phi = N[45.3°,\ 30.4°]$). Without Φ data on free-swimming krill, the latter assumes that the relatively stationary tank populations measured by Kils exhibited the same Φ distributions as potentially more active wild populations. Multi-frequency (e.g. Chu *et al.*, 1993) and broad-bandwidth techniques (e.g. Martin Traykovski *et al.*, 1998) have been suggested for measuring krill-orientation distributions *in situ*, but to date no such data have been published.

In addition to predicting TS(f) for krill, the $SDWBA_{TS}$ can be used for acoustical classification of these important marine organisms. Backscatter at two and three frequencies has been used to classify acoustic backscatter from krill and other sources (e.g. Madureira *et al.*, 1993a, b; Brierley *et al.*, 1998; Demer *et al.*, 1999), but accurate scattering models are required for successful implementations (Greenlaw and Johnson, 1983). Backscatter at three or more frequencies, or over a broad bandwidth, provides even more information for successful taxa classification (e.g. Simmonds *et al.*, 1996; Zakharia *et al.*, 1996). Thus, the $SDWBA_{TS}$ spectra (Figure 6) may improve the accuracy of multi-frequency and broad-bandwidth, echo-trace classification techniques.

Conclusions

A new method for measuring numbers of mobile targets in an echoic cavity from reverberation time-series (De Rosny and Roux, 2001) has been adapted here for accurately and precisely measuring the total sound scatter of swimming krill over a broad bandwidth. With this method, absolute measurements of σ_t of live *Euphausia superba* were obtained conveniently without the usual system calibration. Moreover, the animals' orientations and positions during the measurements were inconsequential. These TTS(f_c) data corroborate the new SDWBA krill-scattering model (Demer and Conti, 2003) by matching the theoretical predictions to better than about 1 dB from f_c=60 to 202 kHz. In this bandwidth, the minor differences in spectrum shapes can be explained by reduced SNR in the lower-frequency measurements. The offset between the TTS measurements and theory (<1 dB) can be explained very easily by measurement error and uncertainties in g, h, and s. Thus, the $SDWBA_{TS}$ may provide the best estimate of TS(f) for *Euphausia superba*, it should aid in the acoustical identification of krill, and it offers reduced measurement error in krill-biomass estimates.

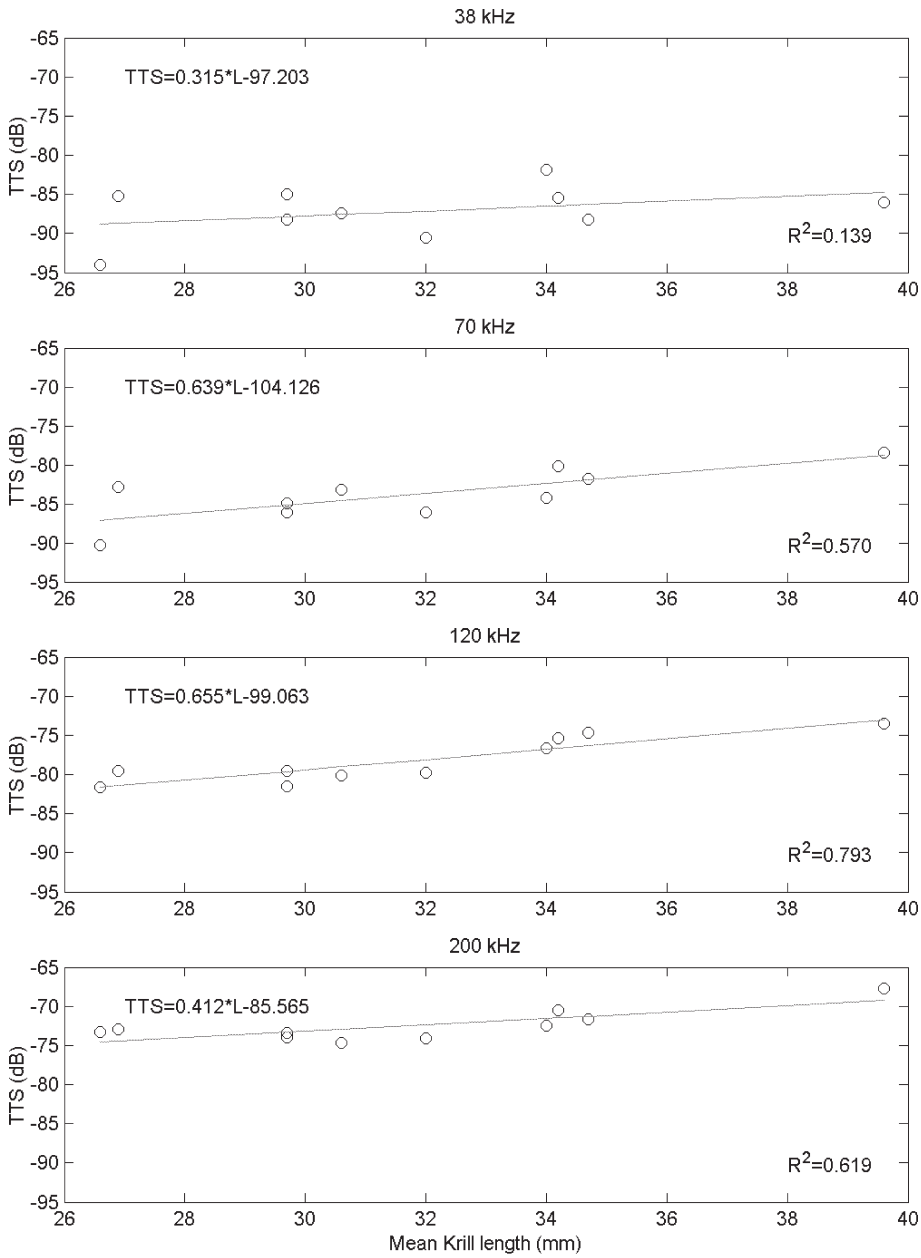

Figure 5. TTS measurements versus mean krill total lengths. For L ranging from 26.6 to 39.6 mm, TTS at 38, 70, 120, and 200 kHz trend upward. At each frequency, there is high variability about the lines fitted to the data and the R^2 values are low. The low slope at 38 kHz is probably an artifact of a low SNR. The slopes are high and similar at 70 and 120 kHz, but decrease at 200 kHz when the wavelength is much smaller than the animal dimensions. Fitting the data to TTS = mlog(L) + b gives similar results: m = 24.251, 47.054, 48.214, and 29.231; b = −123.551, −154.351, −150.516, and −116.286; and R^2 = 0.149, 0.560, 0.778, and 0.565 respectively.

Acknowledgements

We are grateful to the Antarctic Marine Living Resources Division, SWFSC, for funding this investigation. Specific thanks go to Rennie Holt, Director of AERD, for allowing us to conduct the experiments at both the Cape Shirreff field station and aboard the ship. We are grateful also to the AMLR 2002 zooplankton team (Nancy Gong, Emma Bredesen, Shelly Peters, Lorena Linacre-Rojas, Mike Force, Adam Jenkins, Valerie Loeb, and Rob Rowley) for providing us with live animals from the net catches. Rob Rowley was especially helpful in designing and constructing an equipment rack for transporting the electronics to and from the island. Finally, thanks to the team at Cape Shirreff (Iris

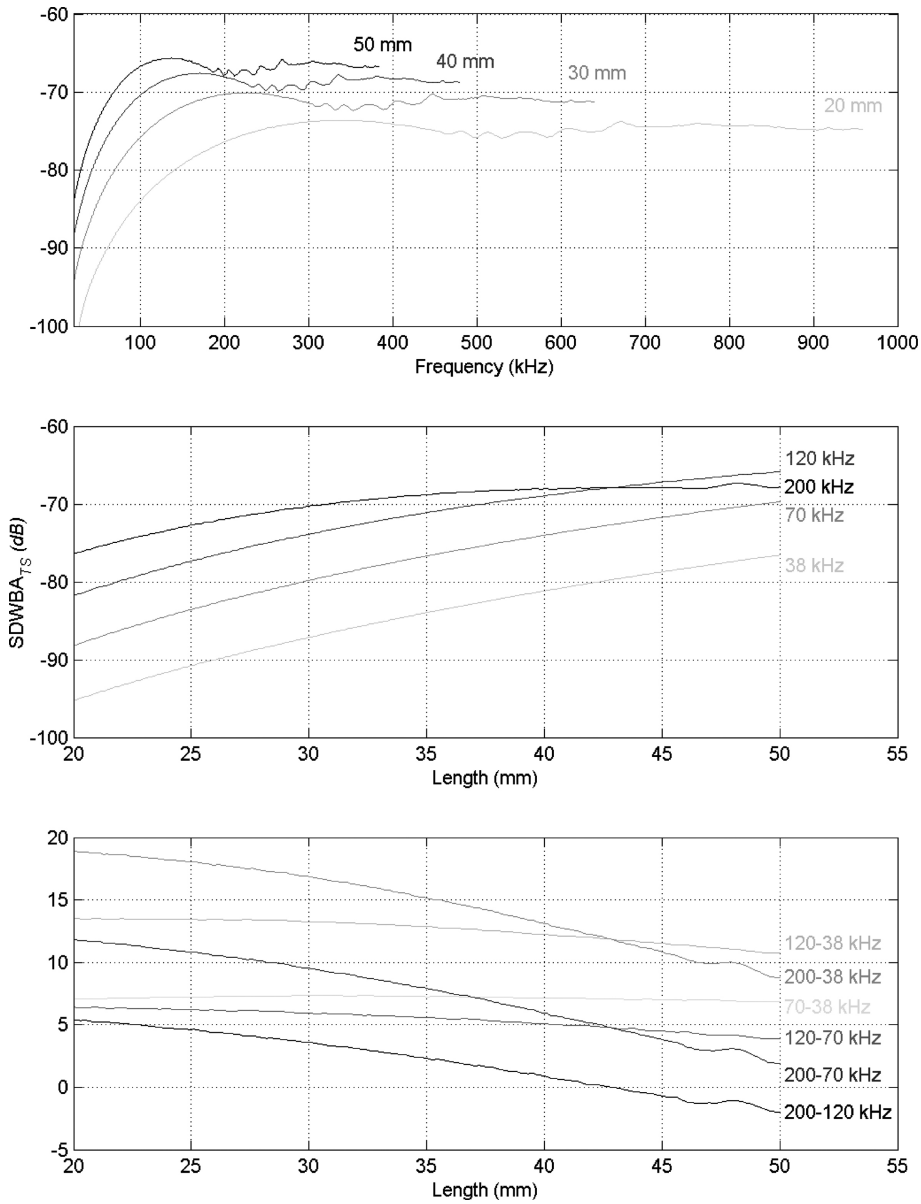

Figure 6. SDWBA$_{TS}$ versus frequency (top panel), and krill length (middle) for four commonly used, echosounder frequencies. The TS(f) spectra (top) and difference in TS at two or more frequencies (bottom) provide information for acoustically identifying Antarctic krill.

Saxon, Brian Parker, Dana Scheffler, Wayne Trivelpiece, and John Lyons) for their hospitality during our stay.

References

Brierley, A. S., Ward, P., and Watkins, J. L. 1998. Acoustic discrimination of Southern Ocean zooplankton. Deep-Sea Research Part II, 45: 1155–1173.

CCAMLR. 1991. Report of the tenth meeting of the scientific committee, 21–25 October 1991. Committee for the Conservation of Antarctic Marine Living Resources, 25 Old Wharf, Hobart, Tasmania 7000, Australia, SC-CAMLR-X.

Chu, D., Foote, K. G., and Stanton, T. K. 1993. Further analysis of target-strength measurements of Antarctic krill at 38 and 120 kHz: comparison with deformed-cylinder model and inference of orientation distribution. Journal of the Acoustical Society of America, 93: 2985–2988.

Demer, D. A. An estimate of error in the CCAMLR 2000 acoustical estimate of krill biomass. Deep-Sea Research Part II, CCAMLR 2000 Special Issue (in press).

Demer, D. A., and Conti, S. G. 2003. Reconciling theoretical versus empirical target strengths of krill; effects of phase

variability on the distorted-wave Born approximation. ICES Journal of Marine Science, 60.
Demer, D. A., and Martin, L. V. 1995. Zooplankton target strength: volumetric or areal dependence? Journal of the Acoustical Society of America, 98: 1111–1118.
Demer, D. A., Soule, M. A., and Hewitt, R. P. 1999. A multiple-frequency method for potentially improving the accuracy and precision of *in situ* target-strength measurements. Journal of the Acoustical Society of America, 105: 2359–2376.
Demer, D. A., Conti, S. G., De Rosny, J., and Roux, P. Absolute measurements of total target strength from reverberation in a cavity. Journal of the Acoustical Society of America 113: 1387–1394.
De Rosny, J., and Roux, P. 2001. Multiple scattering in a reflecting cavity: application to fish counting in a tank. Journal of the Acoustical Society of America, 109: 2587–2597.
Endo, Y. 1993. Orientation of Antarctic krill in an aquarium. Nippon Suisan Gakkaishi, 59: 465–468.
Everson, I., Watkins, J. L., Bone, D. G., and Foote, K. G. 1990. Implications of a new acoustic target strength for abundance estimates of Antarctic krill. Nature, 345: 338–340.
Foote, K. G. 1990. Speed of sound in *Euphausia superba*. Journal of the Acoustical Society of America, 87: 1405–1408.
Foote, K. G., Everson, I., Watkins, J. L., and Bone, D. G. 1990. Target strengths of Antarctic krill *Euphausia superba* at 38 and 120 kHz. Journal of the Acoustical Society of America, 87: 16–24.
Greene, C. H., Stanton, T. K., Wiebe, P. H., and McClatchie, S. 1991. Acoustic estimates of Antarctic krill. Nature, 349: 110.
Greenlaw, C. F., and Johnson, R. K. 1983. Multiple-frequency acoustical estimation. Biological Oceanography, 2: 227–252.
Hewitt, R. P., and Demer, D. A. 1991. Krill abundance. Nature, 353: 310.
Hewitt, R. P., and Demer, D. A. 2000. The use of acoustic sampling to estimate the dispersion and abundance of euphausiids, with an emphasis on Antarctic krill, *Euphausia superba*. Fisheries Research, 47: 215–229.
Kils, U. 1981. The swimming behavior, swimming performance and energy balance of Antarctic krill, *Euphausia superba*. BIOMASS Scientific Series, 3: 122.
Lavery, A. C., Stanton, T. K., McGehee, D. E., and Chu, D. 2002. Three-dimensional modeling of acoustic backscattering from fluid-like zooplankton. Journal of the Acoustical Society of America, 111: 1197–1210.
Madureira, L. S. P., Ward, P., and Atkinson, A. 1998. Differences in backscattering strength determined at 120 and 38 kHz for three species of Antarctic macroplankton. Marine Ecology Progress Series, 93: 17–24.
Madureira, L. S. P., Everson, I., and Murphy, E. J. 1993. Interpretation of acoustic data at two frequencies to discriminate between Antarctic krill (*Euphausia superba* Dana) and other scatterers. Journal of Plankton Research, 15: 787–802.
Martin Traykovski, L. V., O'Driscoll, R. L., and McGehee, D. M. 1998. Effects of orientation on broadband acoustic scattering of Antarctic krill (*Euphausia superba*): implications for inverting zooplankton spectral-acoustic signatures for angle of orientation. Journal of the Acoustical Society of America, 104: 2121–2135.
McGehee, D. E., O'Driscoll, R. L., and Martin Traykovski, L. V. 1998. Effects of orientation on acoustic scattering from Antarctic krill at 120 kHz. Deep-Sea Research Part II, 45: 1273–1294.
Morse, P. M., Ingard, K. U. 1968. Theoretical Acoustics. Princeton University Press, Princeton, NJ. 927 pp.
Ona, E. 1999. Methodology for target-strength measurements. ICES Cooperative Research Report, No. 235. 59 pp.
Simmonds, E. J., Armstrong, R., and Copland, P. J. 1996. Species identification using wideband backscatter with neural network and discriminant analysis. ICES Journal of Marine Science, 53: 189–196.
Wiebe, P. H., Greene, C. H., Stanton, T. K., and Burczynski, J. 1990. Sound scattering by live zooplankton and micronekton: empirical studies with a dual-beam acoustical system. Journal of the Acoustical Society of America, 88: 2346–2360.
Zakharia, M. E., Magand, F., Hetroit, F., and Diner, N. 1996. Wideband sounder for fish-species identification at sea. ICES Journal of Marine Science, 53: 203–208.

Appendix A

$SDWBA_{TTS}$ of Antarctic krill

The following computation was derived from the DWBA (Morse and Ingard, 1968). In Cartesian coordinates, for an incident plane wave in the direction $\vec{k}_i$, a scatterer composed of j-elements, and scattered field in the direction $\vec{k}_s$, the form function for the j-th part of the scatterer is:

$$\phi_{bj}(\vec{k}_i, \alpha, \theta) = \frac{k_1^2}{4\pi} \iiint_V [\nu_\kappa + \nu_\rho \cos\theta] \times \exp(i\vec{\mu} \cdot \vec{r}_0) dV, \quad \text{(A1)}$$

where α and θ are the respective angles in the YZ and XZ planes,

$$\vec{k}_s = \begin{bmatrix} 1 & 0 & 0 \\ 0 & \cos\alpha & \sin\alpha \\ 0 & -\sin\alpha & \cos\alpha \end{bmatrix} \cdot \begin{bmatrix} \cos\theta & 0 & \sin\theta \\ 0 & 1 & 0 \\ -\sin\theta & 0 & \cos\theta \end{bmatrix} \cdot \vec{k}_i, \quad \text{(A2)}$$

$$\vec{\mu} = \vec{k}_s - \vec{k}_i, \quad \text{(A3)}$$

$$\nu_\kappa = \frac{\rho_1 c_1^2}{\rho_2 c_2^2} - 1, \quad \text{(A4)}$$

$$\nu_\rho = \frac{\rho_2 - \rho_1}{\rho_2}, \quad \text{(A5)}$$

ρ is density, c is sound speed, and subscript 1 denotes ambient water and 2 the scatterer.

As in McGehee *et al.* (1998), a krill shape can be approximated by N cylindrical elements of radius a_j positioned along an arc in the XZ plane. In this case, the form function for the j-th cylinder is:

$$\phi_{bj}(\vec{k}_i, \alpha, \theta) = \frac{k_1}{4} \int [\nu_\kappa + \nu_\rho \cos\theta] \exp(i\vec{\mu} \cdot \vec{r}_0) \times \frac{a_j J_1(2k_2 a_j \cos\beta_{tilt})}{\cos\beta_{tilt}} dr_0, \quad \text{(A6)}$$

where $\vec{r}_0$ designates the position of the cylinder axis and β_{tilt} is the incidence angle to the cylinder j. The incident vector orientation is:

$$\vec{k}_i = \begin{bmatrix} \sin\delta \\ 0 \\ \cos\delta \end{bmatrix}. \quad \text{(A7)}$$

The DWBA model assumes a coherent summation of scatter from each of the elements:

$$\phi_b(\delta, \alpha, \theta) = \sum_{j=1}^{N} \phi_{bj}(\delta, \alpha, \theta)\exp(i\varphi_{eq}). \quad \text{(A8)}$$

Demer and Conti (2003) added the phase term to each of the j-cylinders to account for the stochastic nature of sound scattering from krill. For an incident vector orientation δ in the XZ plane, the scattering cross-section is:

$$\sigma(\delta, \alpha, \theta) = \mid \phi_b(\delta, \alpha, \theta) \mid^2. \quad \text{(A9)}$$

The expected value is calculated by averaging $\sigma(\delta, \alpha, \theta)$ over numerous realizations of phase chosen randomly from an expected distribution (e.g. Gaussian distribution of phase jitter due to noise + animal flexure + shape complexity).

The total scattering cross-section (σ_t) is calculated by integrating the square of the form function over all possible incident vectors in the 3D space (i.e. δ), and all refracted angles in the XZ and YZ planes, (i.e. α and θ, respectively):

$$\sigma_t = \frac{1}{2\pi}\int_{\delta=0}^{2\pi} 2 \int_{\alpha=0}^{\pi}\int_{\theta=0}^{\pi} \sin\theta \mid \phi_b(\delta, \alpha, \theta) \mid^2 d\theta d\alpha d\delta. \quad \text{(A10)}$$

Converting to decibels yields the total target strength:

$$\mathrm{TTS} = 10\log_{10}\left(\frac{\sigma_t}{4\pi}\right). \quad \text{(A11)}$$

ICES Journal of Marine Science, 61: 155–156. 2004
doi:10.1016/j.icesjms.2003.12.002

Erratum

ICES Journal of Marine Science, 60: 625–635. 2003☆

Validation of the stochastic distorted-wave Born approximation model with broad bandwidth total target strength measurements of Antarctic krill

David A. Demer and Stéphane G. Conti

In the computations of $SDWBA_{TTS}(f)$ in Figure 4, the scattered vector was integrated over all orientations in the XY plane, where X is the main axis of the krill, but a factor of 2π was erroneously substituted for the numerical integration which accounts for scattering at all angles in the YZ plane. Also, the krill in the study have since been measured to be appreciably fatter than the generic krill shape. In the revised computations and figure, the girth-to-length ratio was 40% larger than that of the generic krill shape, corresponding more accurately to the shapes of the krill in the study, and the scattered vector was integrated over all possible angles in both the XY and YZ planes. The revised Figure 4 is printed below:

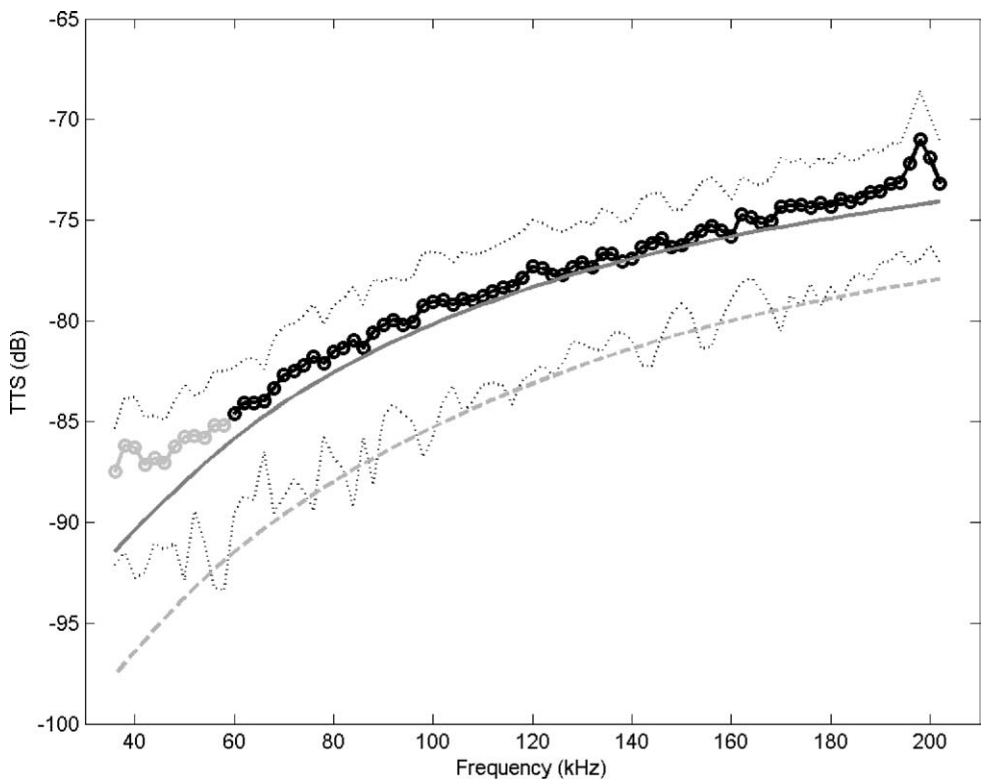

Figure 4. The average TTS of ten aggregations of *Euphausia superba* totaling 57–1169 animals. TTS data from 36 to 60 kHz had low SNRs (gray circles); those above 60 kHz are considered accurate to about 0.4 dB (black circles). The ±1 s.d. error bands (thin dashed lines) encompass the $SDWBA_{TTS}$ predictions (solid gray), computed with $g = 1.0357$, $h = 1.0279$, s with a 40% larger girth-to-length ratio than that of the generic krill shape (consistent with measurements of the krill in this study), and the overall krill length distribution (see Figure 3). The $SDWBA_{TTS}$ computed with the generic s (all other parameters are the same) is also plotted for comparison (thick dashed gray line). Because the random-phase term caused variations in $SDWBA_{TTS}$ of less than 0.1 dB, expected values of TTS were effectively computed at each f using only a single random realization of phase. Error bounds on the prognosticator are thus negligible.

☆ doi of original article 10.1016/S1054-3139(03)00063-8

1054-3139/$30

In Figure 6, the curves were calculated with a generic krill shape that was inappropriately thin, and the $SDWBA_{TS}$ were too large by a factor of 4π. In the revised computations and figure, the girth-to-length ratio was 40% larger than that of the generic krill shape, and the 4π error was corrected. The revised Figure 6 is printed below:

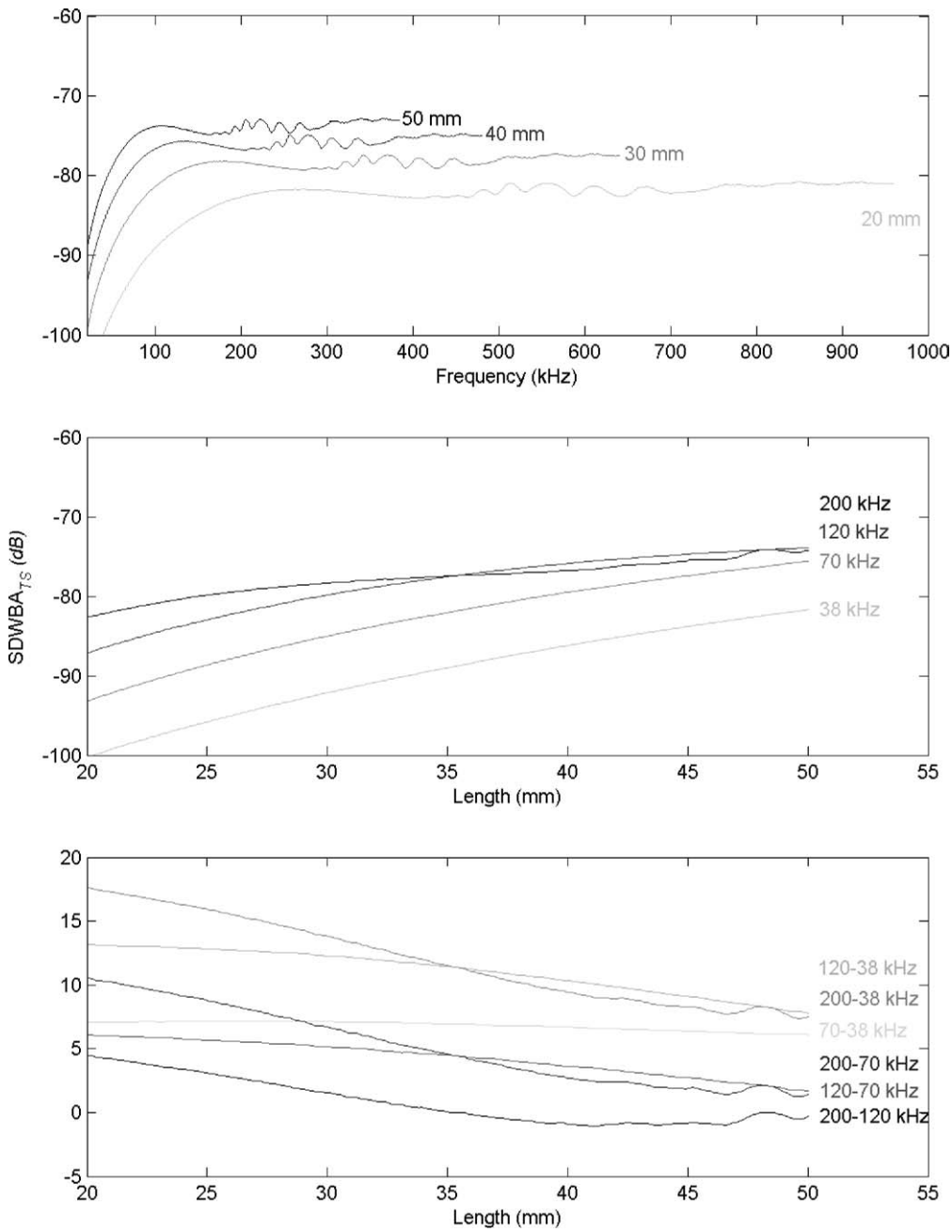

Figure 6. $SDWBA_{TS}$ versus frequency (top panel), and krill length (middle) for four commonly used echosounder frequencies. The TS(f) spectra (top) and difference in TS at two or more frequencies (bottom) provide information for acoustically identifying Antarctic krill.